

MESOSCOPIC WIGNER CRYSTALLIZATION IN TWO DIMENSIONAL LATTICE MODELS

JEAN-LOUIS PICHARD¹, GEORGIOS KATOMERIS^{1,2}, FRANCK SELVA¹

¹*Service de Physique de l'Etat Condensé, CEA - Saclay, 91191 Gif sur Yvette cedex, France*

²*Department of Physics, University of Ioannina, Greece*

The quantum-classical crossover from the Fermi liquid towards the Wigner solid is numerically revisited, considering small square lattice models where electrons interact via a Coulomb U/r potential. The studies of models without disorder and spin and including disorder and spin show that the electron solid is formed in two stages, giving rise to an intriguing solid-liquid regime at intermediate couplings.

1 Lattice model

We consider N electrons on $L \times L$ square lattice with periodic boundary conditions (BCs). The Hamiltonian reads

$$\mathcal{H} = \sum_{i,\sigma} (-t \sum_{i'} c_{i',\sigma}^\dagger c_{i,\sigma} + v_i n_{i,\sigma}) + \frac{U}{2} \sum_{\substack{i,i' \\ i \neq i'}} \frac{n_{i,\sigma} n_{i',\sigma'}}{|i - i'|} + 2U \sum_i n_{i,\uparrow} n_{i,\downarrow}, \quad (1)$$

where $c_{i,\sigma}$ ($c_{i,\sigma}^\dagger$) destroys (creates) an electron of spin σ at the site i and $n_{i,\sigma} = c_{i,\sigma}^\dagger c_{i,\sigma}$. The first terms describe the kinetic energy ($\propto -t$) and the random substrate energy (potentials v_i uniformly distributed inside $[-W/2, W/2]$). The interaction consists of a $U/|i - i'|$ Coulomb repulsion plus a $2U$ Hubbard repulsion. $|i - i'|$ is the smallest distance between the sites i and i' on a square lattice with periodic BCs. In our model, the Coulomb energy to kinetic energy ratio $r_s = U/(2t\sqrt{\pi n_e})$ for a filling factor $n_e = N/L^2$.

S and S_z are the total spin and its component along an arbitrary direction z . \mathcal{H} can be written in a block-diagonal form, with $N + 1$ blocks where $S_z = -N/2, \dots, N/2$ respectively. Assuming $N = 4$ and $L = 6$, the three blocks with $S_z \geq 0$ are diagonalized using Lanczos algorithm to obtain the minimum eigenenergy $E_0(S_z)$ of each block.

2 Spinless fermions without disorder

We begin by studying¹ the ground state (GS) of the block $\mathcal{H}(S_z = 2)$ when $W = 0$. When $U = 0$, the states are N_H plane wave Slater determinants (SDs) $\prod_{p=1}^4 d_{k(p)}^\dagger |0\rangle$, where $d_{k(p)}^\dagger$ creates a particle in a state of momentum $k(p) = 2\pi(p_x, p_y)/L$ and $|0\rangle$ is the vacuum state. The low energy eigenstates are given by: (A) 4 degenerate ground states (GSs) $|K_0(\beta)\rangle$ ($\beta = 1, \dots, 4$) of energy $E_0(U = 0) = -13t$ and of momenta $K_0 \neq 0$; (B) 25 first excitations of energy $E_1(U = 0) = -12t$. (C) 64 second excitations $|K_2(\alpha)\rangle$ of energy $E_2(U = 0) = -11t$; (D) 180 third excitations $|K_3(\alpha)\rangle$ of energy $E_3(U = 0) = -10t$ and (E) 384 fourth excitations of energy $E_4(U = 0) = -9t$. We define the 20 plane wave SDs useful to partly describe the intermediate GS. They are given by 4 plane wave SDs $|K_1(\beta)\rangle$ of energy $-12t$ where the particles have energies $-4t, -3t, -3t, -2t$ respectively, and by 16 plane waves SDs $|K_4(\delta)\rangle$ of energy $-9t$ where the particles have energies $-4t, -3t, -2t, 0t$ (first set of 8 SDs) and $-3t, -3t, -2t, -t$ (second set of 8 other SDs) respectively. Those 20 SDs are directly coupled by the pairwise interaction and their momenta are zero ($K = \sum_{p=1}^4 k(p) = 0$).

When $t = 0$, the states are N_H Slater determinants $c_i^\dagger c_j^\dagger c_k^\dagger c_l^\dagger |0\rangle$ built out from the site orbitals. The low energy states are the following site SDs: (A) 9 squares $|S_0(I)\rangle$ ($I = 1, \dots, 9$)

of side $a = 3$ and of energy $E_0(t = 0) \approx 1.80U$; (B) 36 parallelograms $|S_1(I)\rangle$ of sides $(3, \sqrt{10})$ and of energy $\approx 1.85U$; (C) 36 other parallelograms $|S_2(I)\rangle$ of sides $(\sqrt{10}, \sqrt{10})$ and of energy $\approx 1.97U$ and (D) 144 deformed squares $|S_3(I)\rangle$ obtained by moving a single site of a square $|S_I\rangle$ by one lattice spacing and of energy $\approx 2U$.

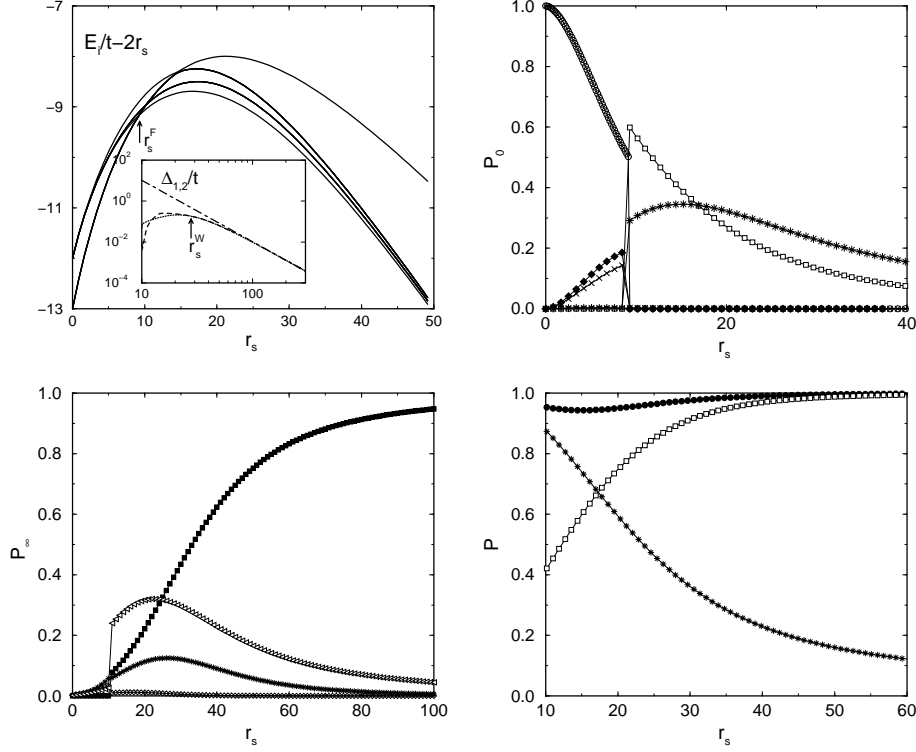


Figure 1: UPPER LEFT: Low energy part of the spectrum exhibiting a GS level crossing at r_s^F . Inset: two first level spacings Δ_1/t (dashed) and Δ_2/t (dotted) which become equal at r_s^W and the perturbative result $\Delta_1/t = \Delta_2/t \approx 10392/r_s^3$ valid when $r_s \rightarrow \infty$ (dot-dashed). UPPER RIGHT: GS projections $P_0(r_s)$ onto a few plane wave SDs, given by the 4 $|K_0(\beta)\rangle$ (empty circle), the 4 $|K_1(\beta)\rangle$ (empty square), the 64 $|K_1(\alpha)\rangle$ (filled diamond), the 180 $|K_2(\alpha)\rangle$ (\times), the 16 $|K_4(\delta)\rangle$ (asterisk) respectively. LOWER LEFT: GS projection $P_\infty(r_s)$ onto a few site SDs, given by the 9 squares $|S_0(I)\rangle$ (filled square), the 36 parallelograms $|S_1(I)\rangle$ (asterisk), the 36 parallelograms $|S_2(I)\rangle$ (diamond), and the 144 deformed squares $|S_3(I)\rangle$ (left triangle) respectively. LOWER RIGHT: GS projection $P_0^t(r_s)$ (asterisk) and $P_\infty^t(r_s)$ (empty square) and total GS projection P (filled circle) onto the re-orthonormalized basis using the low energy eigenvectors of the two limiting bases.

For the first low energy states, the crossover from the $U = 0$ eigenbasis towards the $t = 0$ eigenbasis is shown in Fig. 1 (upper left) when one increases the ratio r_s . If we follow the 4 GSs $E_0(r_s = 0)$ ($K_0 \neq 0$), one can see a first level crossing at $r_s^F \approx 9.3$ with a non degenerate state ($K_0 = 0$) which becomes the GS above r_s^F , followed by two other crossings with two other sets of 4 states with $K_I \neq 0$. When r_s is large, 9 states coming from $E_1(r_s = 0)$ have a smaller energy than the 4 states coming from $E_0(r_s = 0)$. The degeneracies ordered by increasing energy become $(1, 4, 4, 4, \dots)$ instead of $(4, 25, 64, \dots)$ for $r_s = 0$. These 9 low energy states give the 9 square molecules $|S_0(I)\rangle$ when $r_s \rightarrow \infty$. When r_s^{-1} is very small, the first 9 states correspond to a solid molecule free to move on a restricted 3×3 lattice, with an effective hopping term $T \propto tr_s^{-3}$. This gives 9 states of kinetic energy given by $-2T(\cos K_l(I) + \cos K_t(I))$ with $K_l(I) = 2\pi p_l/3$ and $K_t(I) = 2\pi p_t/3$ ($p_{l,t} = 1, 2, 3$). This structure with degeneracies 1, 4, 4 respectively and two equal energy spacings Δ_1 and Δ_2 appears (inset of Fig. 1 upper left) when r_s is larger than the crystallization threshold $r_s^W \approx 28$. The two characteristic thresholds r_s^F (level crossing) and r_s^W (9 first states having the structure of the spectrum of a single solid molecule free to move on a

3×3 square lattice) can also be detected by other methods given in Ref. [1].

To understand further the nature of the intermediate GS between r_s^F and r_s^W , we have projected the GS wave functions $|\Psi_0(r_s)\rangle$ over the low energy eigenvectors of the two eigenbases valid for $U/t = 0$ and for $t/U = 0$ respectively. Let us begin with the $U = 0$ eigenbasis. Below r_s^F , each of the 4 GSs $|\Psi_0^\alpha(r_s)\rangle$ with $K_0 \neq 0$ has still a large projection $P_0(r_s, 0) = \sum_{\beta=1}^4 |\langle \Psi_0^\alpha(r_s) | K_0(\beta) \rangle|^2$ over the 4 non interacting GSs. There is no projection over the 25 first excitations and smaller projections $P_0(r_s, 2)$ and $P_0(r_s, 3)$ over the 64 second and 180 third excitations of the non interacting system. Above r_s^F , the non degenerate GS with $K_0 = 0$ has a large projection

$$P_0(r_s, 1) = \sum_{\beta=1}^4 |\langle \Psi_0(r_s) | K_1(\beta) \rangle|^2 \quad (2)$$

which is equally distributed over the 4 excitations $|K_1(\beta)\rangle$ of momentum $K_1 = 0$ and a second significant contribution

$$P_0(r_s, 4) = \sum_{\delta=1}^{16} |\langle \Psi_0(r_s) | K_4(\delta) \rangle|^2 \quad (3)$$

given by its projection onto the 16 mentioned plane wave SDs $|K_4(\delta)\rangle$ of energy $-9t$. Above r_s^F , its projections onto the 4 $|K_0(\beta)\rangle$, the 21 other first excitations and the second and third excitations of the non interacting system are zero or extremely negligible. The total GS projection $P_0^t(r_s) = P_0(r_s, 1) + P_0(r_s, 4)$ onto the 4 $|K_1(\beta)\rangle$ and 16 $|K_4(\delta)\rangle$ is given in Fig. 1 (lower right) when $r_s > r_s^F$. This shows us that a large part of the system remains an excited liquid above r_s^F .

We now study the GS projections P_∞ onto the $t = 0$ eigenbasis. The GS projection

$$P_\infty(r_s, 0) = \sum_{I=1}^9 |\langle \Psi_0^\alpha(r_s) | S_0(I) \rangle|^2 \quad (4)$$

onto the 9 square site SDs $|S_0(I)\rangle$ is given in Fig. 1 (lower left), together with the GS projection $P_\infty(r_s, J)$ onto the site SDs corresponding to the J^{th} degenerate low energy excitations of the $t = 0$ system. The total GS projection $P_\infty^t(r_s) = \sum_{p=0}^3 P_\infty(r_s, p)$ onto the 9 squares $|S_0(I)\rangle$, the 36 parallelograms $|S_1(I)\rangle$, the 36 other parallelograms $|S_2(I)\rangle$ and the 144 deformed squares $|S_3(I)\rangle$ is given in Fig. 1 (lower right) when $r_s > r_s^F$. This shows us that the ground state begins to be a floppy solid also above r_s^F .

The site SDs and plane wave SDs are not orthonormal. After re-orthonormalization, the total projection P of $|\Psi_0(r_s)\rangle$ over the subspace spanned by the 4 $|K_1(\beta)\rangle$ and 16 $|K_4(\delta)\rangle$ and 225 site SDs of lower electrostatic energies are given in Fig. 1 (lower right), showing that $|\Psi_0(r_s)\rangle$ is almost entirely located inside this very small part of a huge Hilbert space for intermediate r_s , spanned by low energy SDs of different nature, and adapted to describe a solid entangled with an excited liquid.

3 Magnetization and polarization energies in presence of a random substrate

We now consider weakly disordered samples when the spin degrees of freedom are included². Their role and the consequences of an applied parallel magnetic field which aligns only the spins without inducing orbital effects, have been the subject of Ref. [2]. The study of a statistical ensemble of samples with $W = 5$, $N = 4$ and $L = 6$ provides complementary signatures of a particular intermediate behavior. Let us note M the fraction of clusters with $S = 1$ at $B = 0$, $Q_2 = E_0(S_z = 2) - E_0(S_z = 0)$ and $Q_1 = E_0(S_z = 1) - E_0(S_z = 0)$ the Zeeman energies necessary to yield $S = 2$ and $S = 1$ respectively for a cluster with $S = 0$.

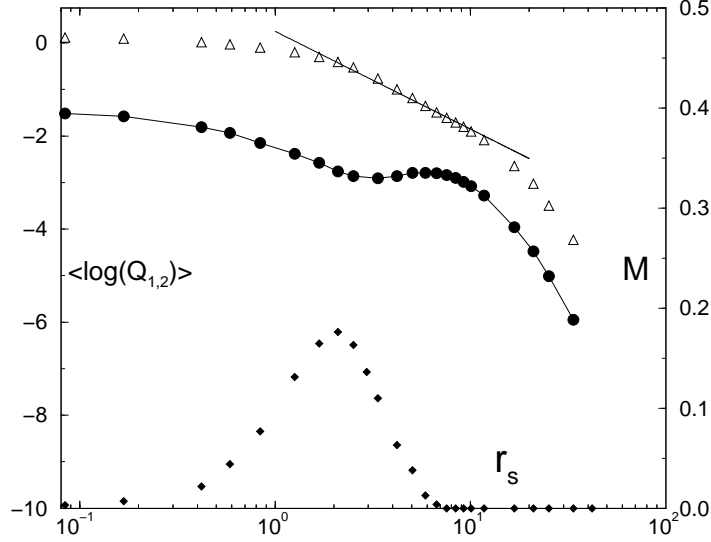


Figure 2: As a function of r_s , fraction M of clusters with $S = 1$ at $B = 0$ (filled diamond, right scale), partial $\langle \log Q_1 \rangle$ (filled circle, left scale) and total $\langle \log Q_2 \rangle$ (empty triangle, left scale) energies required to polarize $S = 0$ clusters to $S = 1$ and $S = 2$ respectively. The straight line corresponds to $0.25 - 2 \log r_s$.

In Fig. 2, M is given as a function of r_s . One can see a first threshold at $r_s \approx 0.35$ where the interaction can drive $S = 1$ in certain samples. Above a second threshold r_s^{FS} , M regularly decreases to reach a zero value at a third threshold $r_s^{WS} \approx 9$ where an antiferromagnetic square molecule is formed. The ensemble averages $\langle \log Q_1 \rangle$ and $\langle \log Q_2 \rangle$ (without taking into account the $S = 1$ spontaneously magnetized clusters) define the typical fields B necessary to yield $S = 1$ or $S = 2$ in a $S = 0$ cluster. In Fig. 2, one can see an intermediate regime again for $r_s^{FS} < r_s < r_s^{WS}$ where $\langle \log Q_1 \rangle$ becomes roughly independent of r_s , while $Q_2 \propto r_s^{-2}$.

4 Conclusion

One concludes that mesoscopic Wigner crystallization proceeds in two stages. In a clean system, a minimal description of the intermediate GS requires to combine the low energy states of the two limiting eigenbases. In this sense, the intermediate GS is neither solid, nor liquid, but rather the quantum superposition of those two states of matter. This is strongly reminiscent of the conjecture proposed by Andreev and Lifshitz³ for the quantum melting of a solid. A path integral Monte Carlo approach⁴ has recently shown that a few electrons confined in a harmonic trap crystallize also in two stages, firstly via a radial ordering of electrons on shells and secondly via the freezing of the intershell rotation. As one can see, a two stage crystallization is not only characteristic of a mesoscopic harmonic trap, but also occurs in a mesoscopic $2d$ torus. To add a random substrate defavors the liquid state. The magnetization gives also the signature of an intermediate regime where Stoner ferromagnetism is defavored by Wigner antiferromagnetism.

References

1. G. Katomeris and J.-L. Pichard, cond-mat/0012213, submitted to *Phys. Rev. Lett.*.
2. F. Selva and J.-L. Pichard, cond-mat/0012015, submitted to *Europhys. Lett.*.
3. A. F. Andreev and I. M. Lifshitz, *JETP* **29**, 1107 (1969).
4. A. V. Filinov, M. Bonitz and Yu. E. Lozovik, *Phys. Rev. Lett.* **86**, 3851 (2001).